J Ther Eng, Vol. 11, No. 2, pp. 476−492, March, 2025

Journal of Thermal Engineering
Web page info: https://jten.yildiz.edu.tr
DOI: 10.14744/thermal.0000928

Research Article

Techno-economic analysis of solar still with nano-phase change material and heating coil: A novel approach for sustainable development

Anand KUSHWAH[1,*], Abdhesh KUMAR[1], M. K. GAUR[2]

[1]*School of Mechanical Engineering, Noida Institute of Engineering Technology, Greater Noida, 201310, India*
[2]*Department of Mechanical Engineering, Madhav Institute of Technology and Science, Gwalior, 474005, India*

ARTICLE INFO

Article history
Received: 19 July 2024
Revised: 03 November 2024
Accepted: 04 November 2024

Keywords:
Economic; Heating Coil; Nanoparticles; PCM; Solar Still

ABSTRACT

A worldwide shortage of drinkable water has resulted from the rapid rise of industrialization and population, prompting researchers to find an alternative method to fulfil this requirement. Solar still systems are powered by solar energy that can provide drinkable water. However, it has a low production issue. This study investigates the performance of two types of solar stills: a conventional solar still and an advanced solar still. Modifications such as an external condenser, a water heating coil, and nano-phase change material (ZnO-PCM) were employed to enhance the productivity of the advanced solar stills. The results demonstrated that the advanced solar still with a heating coil achieved a thermal efficiency of 46% and a yield improvement of 77%, the advanced solar still with an EC achieved a thermal efficiency of 53% and a yield improvement of 119%, and the advanced solar still with ZnO-PCM achieved a thermal efficiency of 51% and a yield improvement of 113%. The productivity of the advanced solar still was enhanced by approximately 36% with ZnO-PCM and by 42% with an external condenser. Economic analysis revealed the cost of desalinated freshwater to be $0.030 per litre for the conventional solar still, $0.023 per litre for the advanced solar still with ZnO-PCM, and $0.021 per litre for the advanced solar still with an external condenser.

Cite this article as: Kushwah A, Kumar A, Gaur MK. Techno-economic analysis of solar still with nano-phase change material and heating coil: A novel approach for sustainable development. J Ther Eng 2025;11(2):476−492.

INTRODUCTION

With the fast rise in population and the growing problem of environmental pollution, there is an urgent need to make natural water safe for people to use. As water treatment requires significant energy, and due to the recent increases in conventional fuel costs, there is a growing necessity to explore alternative energy sources. Solar energy, which is both clean and sustainable, is becoming a popular choice for various applications [1]. One effective application is the use of single-slope solar distillers for desalinating water, providing an easy and efficient method for producing clean drinking water. On Earth, only 2.7% of water is fresh and accessible through rivers, lakes, and groundwater. The World Health Organization asserts that

***Corresponding author.**
*E-mail address: anand.kushwah@niet.co.in

This paper was recommended for publication in revised form by Editor-in-Chief Ahmet Selim Dalkılıç

drinking water must be safe for all ages. In India, however, increasing population and industrial activity are expected to make access to clean water more challenging, leading to water shortages in both urban and rural areas. Addressing this issue requires affordable water treatment technologies that comply with Environmental Protection Agency guidelines. Among the available options, solar stills stand out for their low construction costs and zero electricity requirements, though their yield remains limited. Researchers are working to improve the efficiency of solar stills to better meet the demand for safe drinking water [2].

For numerous developed and emerging countries, freshwater scarcity is increasingly viewed as a primary concern, exacerbated by ongoing population growth, industrialization, and agricultural development. It is projected that by 2030, there will be a 40% reduction in freshwater resources. Solar energy serves as a principal renewable energy source for a variety of applications, including electricity generation, water desalination, water and air heating, solar drying, and solar cooking. Distillers provide several notable advantages for remote and island locations where the high cost of transporting filtered water, due to a lack of freshwater resources, is a significant issue. It is more economical to design a distillation system that utilizes readily available materials, is low-maintenance, and supports environmentally friendly infrastructure. Solar stills are an effective technique for harnessing solar energy for water purification. They offer two primary benefits: they are relatively simple and safe to operate, and they are environmentally friendly. By using solar energy, they reduce reliance on fossil fuels and hazardous materials, which in turn lowers global warming emissions. Nevertheless, a significant drawback of solar stills is their lower efficiency compared to other desalination methods, producing only 2–5 litres of purified water per square meter per day in basic models. The reliance on traditional energy sources has posed substantial energy challenges in recent decades, making solar stills a practical solution for providing fresh water to small, isolated communities.

A no. of studies has been carried out to improve the productivity as well as thermal efficiency of SS systems [3, 4]. Numerous solar still system geometries, such as stepped solar still [5], [6], half barrel solar still [7], pyramid solar still [8, 9] conventional solar still [10-13], trays solar still [14], single slope solar still [15-19], double slope solar still [20], and tubular solar still [21] have been put to the test in a variety of design and operating scenarios. In addition, the performance of solar still systems has been improved by the introduction of reflectors [22], nanoparticles [10], phase change material [23], wick material [24], fins [25], and spinning components [6]. Andre et al. created a thermal model to optimize and predict performance of solar stills, testing ideas for improving efficiency by examining factors like wall design and shadowing effects. Their findings showed that conventional solar stills performed significantly better with reduced water depth, increased wall height, enhanced insulation, and the addition of reflectors [26]. Dumka et al. improved the performance of conventional solar still employing 100 cotton sacks packed with sand at different water depths. Outcomes of this research indicated that CSS has more productivity (31%) using sandbags compared to general CSS [27]. Dumka et al. evaluated the theoretical as well as practical study on CSS using fixed ring magnets. The results demonstrated that CSS has more productivity (49%) using permanent magnets than CSS [28]. Panchal et al. evaluated the thermal performance of CSS using mixture of carbon powder and black paint at various concentrations. As the concentration of carbon powder varied in the range of 20-40%, the productivity also improved in the range of 10.5-17%. Due to this concept, water temperature increases and heat transfer rate also increases [29]. Panchal et al. developed an advanced single slope solar still coupled with ETSC and small calcium stones also used [30]. The experimentation procedure was categorized in two cases: In Case-I solar still assisted with ETSC and Case-II solar still coupled with ETSC using calcium stones. The findings indicated that productivity of SS increases as 114% and 105% in both cases respectively. Also, SS yield improved by 20% by using rock stone bed, which act as an energy storing devices. Murugavel and Srithar fabricated a novel double slope basin type SS using different wick materials as well as aluminium fins. It was observed that large quantity of mass distillate produced using light black cotton cloth [31]. Alawee et al. investigated a double slope solar still with elevated basin [32]. Multiple approaches are used to make a profit from solar intensity that hits the back wall of solar still. Younes et al. evaluated the performance analysis of corrugated absorber as well as half-barrel absorber solar still using wick material on side walls of SS. Purpose of wick material to enhance surface area at where water evaporates and protects side walls of solar still from direct beam radiation. Due of which, rate of evaporation and condensation improved whereas rate of heat losses decreased. It was noted that corrugated SS and half-barrel SS had per day yield 139% and 154% respectively more compare to CSS [7]. Elamy et al. investigated various methods to enhance the performance of a coiled solar still (COSS). One key approach involved the addition of a vertical wick distiller (VWSS) equipped with built-in reflectors positioned downstream from the COSS. The findings highlighted substantial improvements in distillate production resulting from these modifications. The COSS alone demonstrated a 76% increase in daily output compared to a conventional solar still (CSS). When a heating coil and internal reflectors were incorporated, productivity surged by an impressive 92%. This configuration exhibited a remarkable 209% increase in distillate production relative to the CSS, a figure that soared to 269% with the inclusion of a heating coil, VWSS, and an external condenser. The addition of a fan to the MCOSS further enhanced efficiency to 68%. Notably, incorporating nanomaterial-infused paraffin wax (PCM-Ag) with the MCOSS featuring the VWSS resulted in a striking 246% increase in productivity compared to the standard design. Additionally, the research indicated a significant reduction in the cost of freshwater production, with the cost per litre determined to be $0.024 for the CSS and a substantially lower $0.0126 for the MCOSS with a fan [33].

Essa et al. developed a new system in which a rotating disc fitted on back side wall of CSS. The whole experimentation work was carried out in two phases. In Phase-I the rotating disc is used with wick material, while in phase-II, the rotating disc is used with wick material. Results demonstrated that corrugated disc SS with wick material produced 124% more drinkable water [34]. Nakade A et al. developed a system that integrates an evacuated tube solar collector (ETSC) with a thermal energy storage (TES) system, utilizing pure paraffin wax and nano-enhanced phase change materials (NEPCM) for desalination. This innovative setup incorporates two water tanks linked to the ETSC, allowing for a two-phase system that effectively doubles the water output. The PCM section is filled sequentially: initially with pure paraffin wax, followed by the addition of NEPCM, which consists of paraffin wax infused with aluminium oxide (Al_2O_3). This configuration enables the water tank to be heated to temperatures ranging from 54 to 128 °C. The results demonstrate a significant increase in freshwater yield, with an enhancement of 60.09% achieved through the use of NEPCM compared to pure paraffin wax in the TES. Additionally, energy efficiency saw a notable improvement of 49.91% with NEPCM over the conventional paraffin wax [35]. Younes et al. evaluate the effect of 04 rotating discs on SS's side and back wall. Finned shape discs give better SS results than corrugated and flat-type discs. The yield enhancement over CSS for finned type, flat type, and corrugated type disc SS was 106%, 68%, and 86%, respectively [36]. Abdullah et al. modified the CSS by implementing the internal trays on rear side wall. It was observed that 95% more drinkable water was produced in trays SS using internal and external reflectors compared to CSS. Also, the yield of SS can be achieved 108% more than CSS by increasing the trays [37]. Abdullah A.S et al. examined how various modifications impacted the performance of a half-cylindrical solar still (HCYSS). By comparing each modification's distillate yield to a baseline, the research found that the HCYSS outperformed CSS by 55%. Key enhancements included a convex surface absorber, which boosted yield to 6300 ml/m²- 94% higher than the CSS's 3250 ml/m². The corrugated convex design further increased yield by 123%. The most significant improvement came from combining a reflector and PCM-Ag composite, achieving a remarkable 184% increase in productivity and an efficiency of 61.5%. These results suggest that the HCYSS's optimized design could significantly enhance solar desalination efficiency [38].

A comprehensive review of previous research highlights that while several strategies have been developed to enhance the solar intensity on the back wall of solar stills, including rotating discs, vertical wicks, and trays, there has been no investigation into the specific processes of heating and condensation on the back wall itself. This experiment introduces a novel approach by delivering cold feed water through a copper coil attached to the back wall to enhance condensation and increase the temperature of the feed water. By lowering the back wall's temperature with the copper coil heater, the experiment effectively minimizes heat loss to the surrounding air. The study also examines the impact of combining a Phase Change Material (PCM) bed with ZnO nanoparticles, as well as the use of an external condenser with an electric fan.

MATERIALS AND METHODS

This section covers the details of the fabrication and installation processes as well as the experimental procedures implemented.

Material Used

For the experiment, a 2 mm thick stainless-steel sheet (thermal conductivity of 58 W/m²K, density 7.80 g/cm³), 20 mm thick plywood, and 20mm thick polystyrene (thermocol) were procured from the local market in Gwalior, M.P., India. The system was enclosed using 4mm thick toughened glass, and a condenser was constructed on the back wall of the solar still using a 5mm diameter copper tube.

Methodology

In the current research, two different types of solar still (SS) systems were developed at the Solar Energy Lab of Madhav Institute of Science & Technology, Gwalior, India. The first type is a conventional solar still (CSS), while the second is an advanced solar still (ASS), as depicted in Figures 1 and 2. The CSS is constructed using a 2mm thick stainless-steel sheet, with a detailed description provided in Table 1. The system is enclosed with a 4mm thick toughened glass that acts as a condensing surface. To collect the condensate water, an inclined trough is attached to the lower edge of the solar still. The ASS is designed similarly to the CSS but includes several modifications, classified into three categories.

Category I: A copper tube heater (5m length and 5mm diameter) is integrated. This copper coil also functions as a condenser since cold water entering it condenses some of the steam. An inclined trough beneath the copper coil on the back wall of the solar still collects the condensate.

Category II: To enhance the SS yield, a 6-watt, 100mm diameter DC fan is mounted on the rear wall of the SS to extract steam to an external condenser, thereby improving the condensation process.

Category III: A 20mm PCM-ZnO nanoparticle layer is added underneath the absorber plate. Additionally, the interior and exterior of the SS system are painted black to increase solar absorptivity.

The primary objective of this study is to install a copper tube heater on the back wall of the CSS to preheat the feed water before it enters the SS. This installation also reduces the back wall temperature, minimizing heat loss to the surrounding air. The use of the copper heating coil increases the evaporation and condensation rates, raising the temperature of the glass covers. To lower the glass temperature and enhance production, two strategies were employed:

Fan extraction: Steam is extracted from the distiller using a fan and condensed inside the feeding tank, thereby increasing the temperature of the feed water and helping to decrease the glass cover temperature.

Table 1. Detailed description of experimental setup

Component	Description
Solar still	
Plywood	20mm (Thickness)
Thermocol	20mm (Thickness)
Steel sheet	2mm (Thickness)
Glass cover	4mm (Thickness)
Iron stand	02 ((Thickness 5mm)
Basin area	1m × 1m
Lower height	0.2m
Height of back wall	0.7m
Inclination angle	26°
Latitude of site location	26.2183° N, 78.1828° E
DC fan	
Types	06 W DC solar powered
Copper tube	
Length of copper tube heater	4m
Diameter of copper tube	5mm
Thickness of PCM-ZnO layer	20mm

PCM-ZnO nanoparticle layer: A 20mm PCM-ZnO nanoparticle layer is placed underneath the absorber plate.

In present study, we focused on the physical principles underlying the operation of the system, particularly the thermal dynamics involved in the phase change materials

Figure 1. Actual picture of experimental setup.

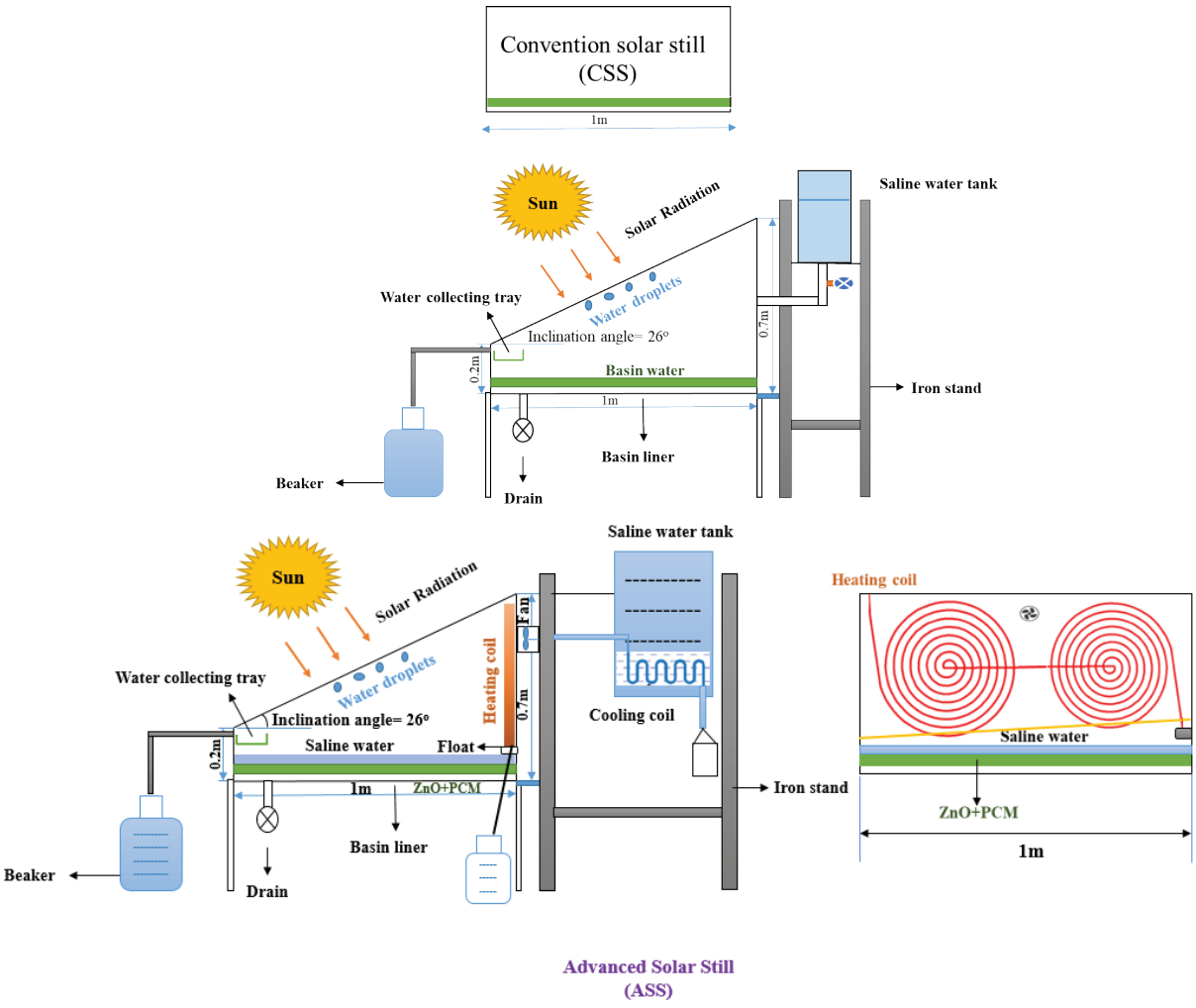

Figure 2. Schematic diagram of experimental setup.

Table 2. Description of instruments and uncertainty

Used measuring devices	Accuracy	Ranges	Standard uncertainty (σ)	Uncertainty of observed parameters
K-types thermocouple (PT-100 and PT-1000 sensor)	±0.1°C	-140 to 990°C	0.0567°C	±0.265v
Infrared Temperature gun (HTC, MTX-2)	±1°C	-40 - 500°C	1.143°C	±1.175
Solarimeter (PMV-210)	11 W/m^2	0-2000W/m^2	5.67 W/m^2	5.67 W/m^2
DYNALAB DLAW-8701 Digital Anemometer	±1m/s	0-45m/s	0.566m/s	0.645m/s
MEXTECH TM-1 Digital Hygrometer	2%	5-85%	1.72%	1.69%
Graded bottles	0.2l	0.01l		0.2l

and the role of ZnO nanoparticles in enhancing the thermal conductivity.

Thermal dynamics

The PCM bed functions by absorbing excess thermal energy during the day and releasing it when needed, thus improving the system's efficiency. The phase transition of the PCM is critical, as it allows for efficient energy storage and management, which is crucial for maintaining optimal operation during periods of low solar irradiance.

Role of ZnO nanoparticles

ZnO nanoparticles contribute to increased thermal conductivity and enhanced heat transfer rates. Their presence in the working fluid helps facilitate faster evaporation rates, improving the overall efficiency of the desalination process. A physical discussion of how the size, shape, and concentration of ZnO nanoparticles impact heat transfer can provide valuable insights.

External condenser dynamics

The design and operation of the external condenser, coupled with the electric fan, play a significant role in maximizing condensation efficiency. The fan increases air circulation, promoting more effective heat exchange, which can lead to higher water collection rates.

Experimental observations

We will include a more detailed analysis of experimental observations related to thermal performance, evaporation rates, and overall system efficiency, including how these parameters interact within the physical framework of the system.

Instrumentation for Recording Observations

- A data logger (Data Taker DT85 series 3, Australia) is installed to record relative humidity (Rh) and ambient air temperature. The experimental work is conducted from 10:00 to 18:00 hours.
- An anemometer (Dynalab DLAW 8701) is used to measure the airflow rate (m/s) over the glass covers of both the CSS and ASS.
- A solarimeter (Megger PVM 210) is mounted to record direct beam radiation and diffused solar radiation at regular intervals.
- K-type thermocouples are used to record the temperature at different locations of the SS (CSS and ASS).

Uncertainty Estimation

Table 2 provides details on the instruments used for evaluating ambient air properties, including their accuracy, range, standard uncertainty, and the uncertainty in the measured variables.

If X_1, X_2……X_n are the independent variables affecting the observed parameter Y, uncertainty in observed variable U(Y), is computing using Eq. 1[39]:

$$U(Y)=\left[\left(\frac{\partial Y}{\partial x_1}\right)^2 u^2(x_1)+\left(\frac{\partial Y}{\partial x_2}\right)^2 u^2(x_2)+\cdots\ldots\ldots+\left(\frac{\partial Y}{\partial x_n}\right)^2 u^2(x_n)\right]^{1/2} \quad (1)$$

Where, U(Y) is the total uncertainty, $u^2(x_1)$, $u^2(x_2)$, …., $u^2(x_n)$ are uncertainties of independent variables.

Thermal Efficiency of the System

The thermal efficiency of a solar still system can be computed by following relations.[40]:

$$\eta_d = \frac{\sum m \cdot \times h_{fg}}{\sum A \times I + P_F} \quad (2)$$

Latent heat of vaporisation according to water temperature can be determined as [41]:

$$h_{fg}=3.1625\times10^6+[1-(7.1616\times10^{-4}\times T_w)] \text{for } T_w>70°C \quad (3)$$

$$h_{fg} = 2.4935 \times 10^6[1-(9.4779\times10^{-4}\times T_w) +(1.3131\times10^{-7}\times T_w^2)-(4.7974\times10^{-9}\times T_w^3)] \quad (4)$$
$$\text{for } T_w < 70°C$$

Economic Analysis

The objective of system modification is to lower production costs while also increasing water productivity. Various factors, including setup size and design, insulation

and fabrication materials used in SS, site location, labour costs, and feed water quality, raise the cost of producing SS water. [15].

Capital recovery factor (CRF) can be evaluated as follows:

$$\mathrm{CRF} = \frac{\mathrm{i}(1+\mathrm{i})^{\mathrm{n}}}{[(1+\mathrm{i})^{\mathrm{n}}-1]} \quad (5)$$

While F = current capital cost, therefore the fixed annual cost (FAC) and Annual salvage value (ASV) can be calculated as:

$$\mathrm{FAC} = \mathrm{F(CRF)} \quad (6)$$

Further, current capital cost (F) can be rewritten as:

F=Cost of system+Cost of Nanopartcles+Cost of all needed deviesc+Labour cost (7)
ASV=(SFF)S

The value of S =0.2F, SFF= Sinking fund factor and can be determined using Eq. 8

$$\mathrm{SFF} = \frac{\mathrm{i}}{[(1+\mathrm{i})^{\mathrm{n}}-1]} \quad (8)$$

Total yearly expense (TAC) can be computed using the following relations:

$$\mathrm{TAC} = \mathrm{FAC} + \mathrm{AMC} - \mathrm{ASV} \quad (9)$$

Therefore, AMC = Costs of yearly upkeep, which includes the cost of paint, labour cost, sealing material cost, and all breakdowns cost. That measured to be 15% of FAC. It may be written as[15]:

$$\mathrm{AMC} = 0.15\mathrm{FAC} \quad (10)$$

The price of distilled water per litre (CPL) can be computed as:

$$\mathrm{CPL} = \frac{\mathrm{TAC}}{\mathrm{M}} = \frac{\text{Total yearly expense}}{\text{Total yearly yield}} \quad (11)$$

The time consumed by the experimental setup to return the invested cost is known as the payback period. The payback period (n_p) For the advanced system is calculated as:

$$n_p = \frac{ln\left(\frac{M_y \times S_p}{(M_y \times S_p)-(CC \times i)}\right)}{ln(1+i)} \quad (12)$$

Nano fluid Preparation

Nanoparticles are hydrophobic by nature. To make them hydrophilic, certain methodologies have been implemented.

Synthesis of ZnO nanoparticles

ZnO nanoparticles were synthesized using a sol-gel method. This involved dissolving zinc acetate in a solvent, typically ethanol, followed by the addition of a stabilizing agent, such as polyvinyl alcohol (PVA), to prevent agglomeration during the formation process. The solution was stirred and heated to promote the formation of ZnO.

Preparation of ZnO nano fluid

The ZnO nanoparticles were then dispersed in a base fluid, such as distilled water or ethylene glycol. A surfactant was added to enhance stability and prevent sedimentation. The mixture was subjected to ultra-sonication for a specific period to achieve a uniform dispersion of the nanoparticles within the fluid.

Stability testing

To ensure the stability of the ZnO Nano fluid, zeta potential measurements were conducted. A zeta potential greater than ±30 mV indicates good stability, which minimizes the risk of agglomeration over time.

Homogeneity check

Visual inspection and sedimentation tests were performed periodically to check for any signs of agglomeration or settling of the nanoparticles.

Figure 3 illustrates the steps involved in the preparation of Nano fluids. It has been observed that most researchers use surfactants and dispersants to make nanoparticles soluble in water.

The presence of surfactants and dispersants raises the boiling point of water, causing it to evaporate more slowly. The detailed specification of ZnO nanoparticles is given Table 3. Concentration of nanoparticles is determined using Eqs.13-14 [15].The selection of ZnO nanoparticles in the current work, due to their exceptional photocatalytic properties, high thermal conductivity, and stability under UV and visible light. ZnO nanoparticles enhance the evaporation rate by efficiently absorbing solar energy and converting it into heat. Additionally, they help improve the overall efficiency of water purification by breaking down contaminants through photo catalysis, making the desalination process faster and more effective.

$$\varphi_{np} = \left({}^{m_{np}}/_{m_{np}+m_w}\right) \times 100 \quad (13)$$

Constitutive equation

The constitutive equation for Nano fluids is an extension of the classic fluid mechanics equations, incorporating the effects of the dispersed nanoparticles. One commonly used model to describe the effective thermal conductivity k_{nf} of a Nano fluid is given by the following equation:

$$k_{nf} = k_b\left(1 + \frac{3\emptyset}{(1-\emptyset)}\left(\frac{k_{p-}\, k_b}{k_p+2k_b}\right)\right) \quad (14)$$

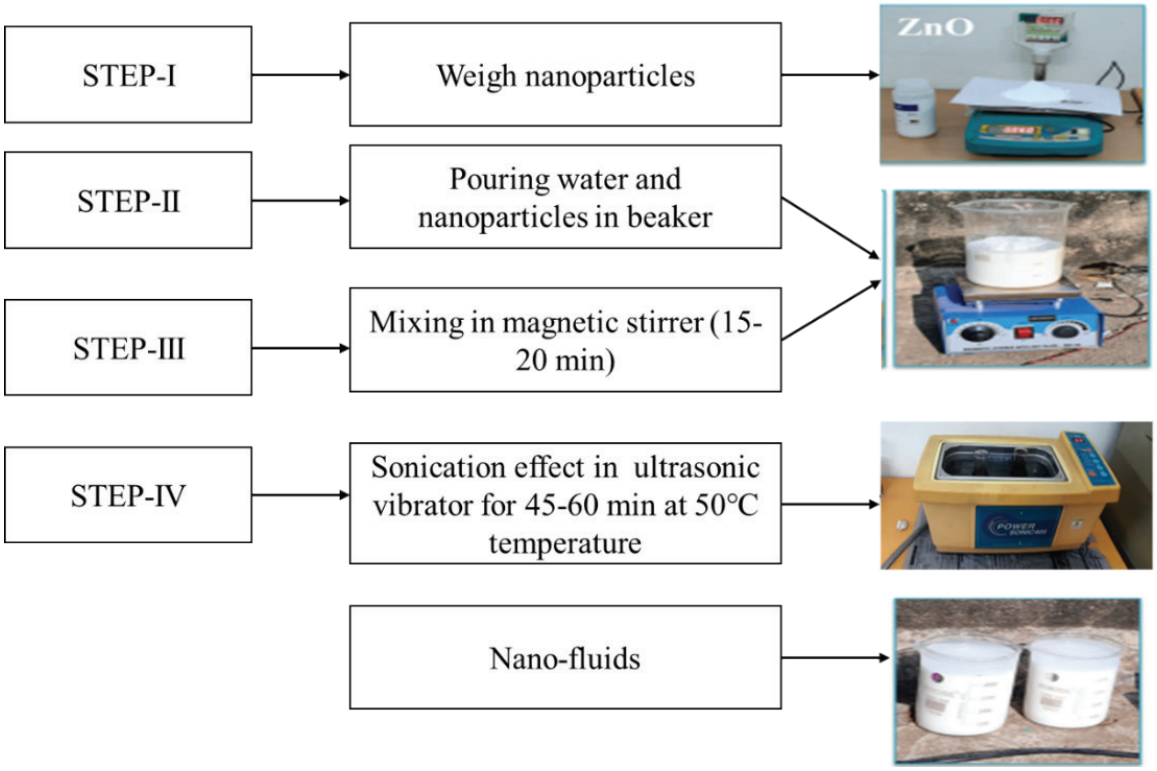

Figure 3. Layout diagram of nano fluids preparation.

Table 3. Specification of ZnO nanoparticle

Nanoparticles	Thermal conductivity (W/mK)	Density (kg/m^3)	Size of particle (nm)	Appearance	Specific heat (J/kg K)
ZnO	6.5	6000	30-50	White	443.4

Where:
k_{nf} = effective thermal conductivity of the Nano fluid.
k_b = thermal conductivity of the base fluid.
k_p = thermal conductivity of the nanoparticles.
ϕ = volume fraction of the nanoparticles.

This equation accounts for the interactions between the base fluid and the nanoparticles, providing a means to predict the thermal conductivity of the resulting Nano fluid based on the properties of the individual components. Additionally, other properties such as viscosity and specific heat may also need to be modified based on the concentration and type of nanoparticles used, leading to further constitutive relations for those properties.

RESULTS AND DISCUSSION

A copper heating coil is employed to elevate the feed water temperature, enhancing vaporization and condensation rates without enlarging the projected area of the solar still. The effects of incorporating a DC fan, EC, and PCM will also be discussed in subsequent sections. Various parameters were recorded during the experimentation, including solar radiation, yield of potable water, airflow velocity, and temperatures at different locations (glass cover, basin, PCM, and water). Origin Pro 2024b was used to draw graphs.

Performance Analysis of ASS Using Heating Coil (ASS)

The performance evaluation of ASS has been compared with that of CSS. Figures 4 and 5 indicate the hourly variation in solar intensity, glass cover temperature, air temperature, and basin water temperature (BWT). Average water temperature difference b/w ASS and CSS was noted as 0-12°C. It is because of copper heating coil that water is automatically fed into the ASS, and it is also observed that feed water temperature is higher in the range of 0-10°C as compared to conventional SS. It is necessary to know that the feed water of CSS is approximately at room temperature. Maximum water temperature and glass cover temperature were recorded as 75°C & 55°C and 63°C &

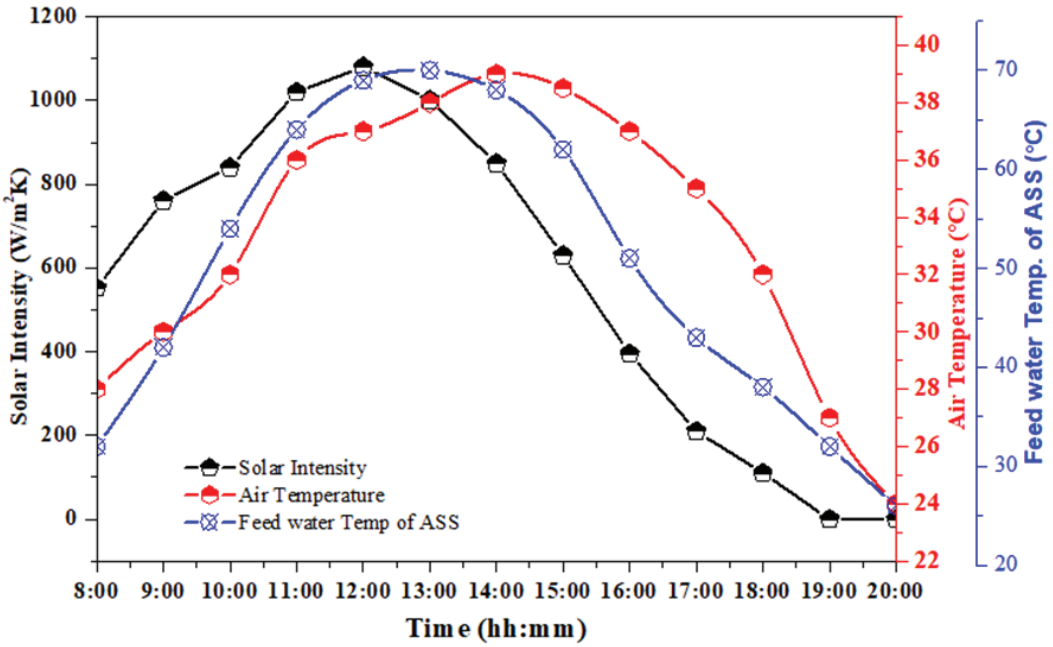

Figure 4. Variation in solar radiation, ambient temperature, and temperature of feed water for CSS and ASS (with heating coil).

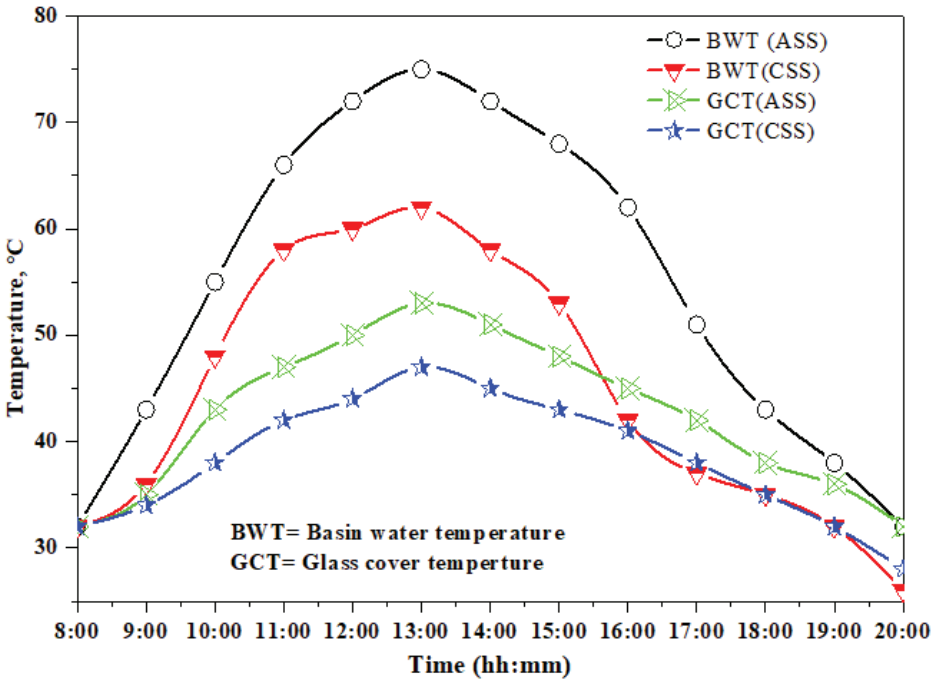

Figure 5. Variation in basin water and glass cover temperature with the time of day for both systems.

47°C in ASS and CSS, respectively, at 13:00h. Similarly, higher feed water temperature of ASS was noted as 72°C at13:00h. Glass cover temperature for ASS revealed higher values than that for conventional SS by around 0 - 7°C due to higher evaporation and condensation rates for ASS compare to CSS as a result of more water temperature for ASS. From Figure 4, it was observed that the solar intensity fluctuated in the range of 0- 1070W/m^{2}K. The maximum solar radiation was noted as 1070W/m^{2}K at 12:00h and started decreasing.

The hourly variations in yield between advanced SS and conventional SS were compared and are shown in

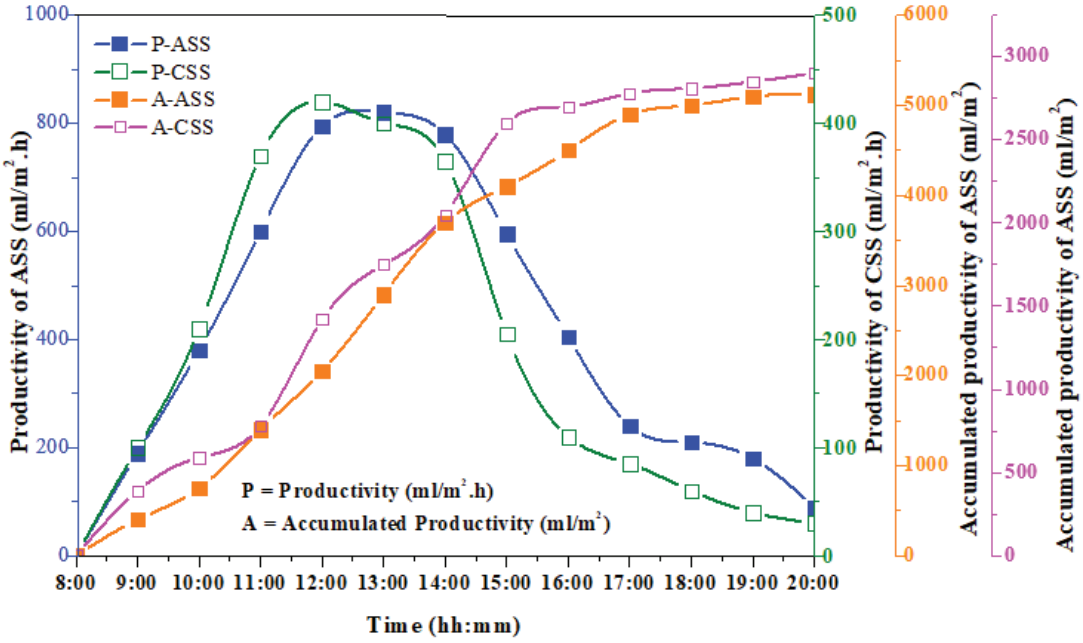

Figure 6. Hourly variation in productivity and accumulate productivity for ASS and CSS.

Figure 6. The graph illustrates that advanced SS consistently outperforms conventional SS in daily productivity. This superiority can be attributed to higher rates of BWT, evaporation, and condensation in advanced SS compared to conventional SS. At 13:00h, the maximum fresh water yield reached 860 ml/m² and 485 ml/m² for advanced SS and conventional SS, respectively. Over the course of the period, advanced SS achieved a cumulative yield of 5500 ml/m², which is nearly 77% higher than the 3090 ml/m² achieved by conventional SS, as depicted in Figure 7. The present study results are much better compare to previous work conducted by Elamy et al. [33]. The COSS alone demonstrated a 76% increase in daily output compared to a conventional solar still (CSS). When a heating coil and internal reflectors were incorporated, productivity surged by an impressive 92%.

Performance Evaluation of ASS with Heating Coil and External Condenser (ASS-EC)

The temperature of the glass covers in advanced solar still (ASS) has been reduced using an axial DC fan and an external condenser to improve the condensation process. By employing an external condenser with heating coils, the glass cover temperature and basin water temperature of ASS can be increased by 0-2°C and 0-7°C, respectively, compared to conventional solar stills (CSS). The suction fan in ASS-EC lowers the internal pressure, thereby reducing the temperature of salt water. Additionally, the suction fan directs most of the water vapour inside ASS towards the external condenser (EC). This process results in the condensation of low-temperature water vapour on the inner surface of the glass cover. Figures 7 and 8 illustrate the hourly variations in solar intensity, glass cover temperature, air temperature, and basin water temperature (BWT), respectively.

Additionally, it was noted that the solar intensity fluctuated in the range of 0-1090W/m²K. The maximum solar radiation was noted as 1070W/m²K at 12:00h and started decreasing. Higher water temperature and glass cove temperature were achieved as 71°C & 51°C and 62°C & 47°C in ASS-EC and CSS, respectively, at 13:00h. It was also observed that maximum basin water temperature (69°C) attained in ASS at13:00h and after that begins to go down.

The variation of hourly yield for ASS-EC and CSS has been compared and displayed in Figure 9. The yield of fresh water reached 7000 ml/m² and 3200 ml/m² per day in ASS-EC and CSS, respectively, at 13:00h. Hence, ASS-EC has a 119% more distillate production compared to CSS. As a result, the productivity of ASS has increased by about 42% employing the EC. This is mostly because having fan increases productivity and the suction fan, which circulates air inside the solar still above the salty water, accelerates evaporation by creating some turbulence. Furthermore, the suction fan draws most of the vaporised water from the saline water into EC. The current works finds are in the same with literature work. When a heating coil and internal reflectors were incorporated, productivity surged by an impressive 92%. This configuration exhibited a remarkable 209% increase in distillate production relative to the CSS, a figure that soared to 269% with the inclusion of a heating coil, VWSS, and an external condenser [33].

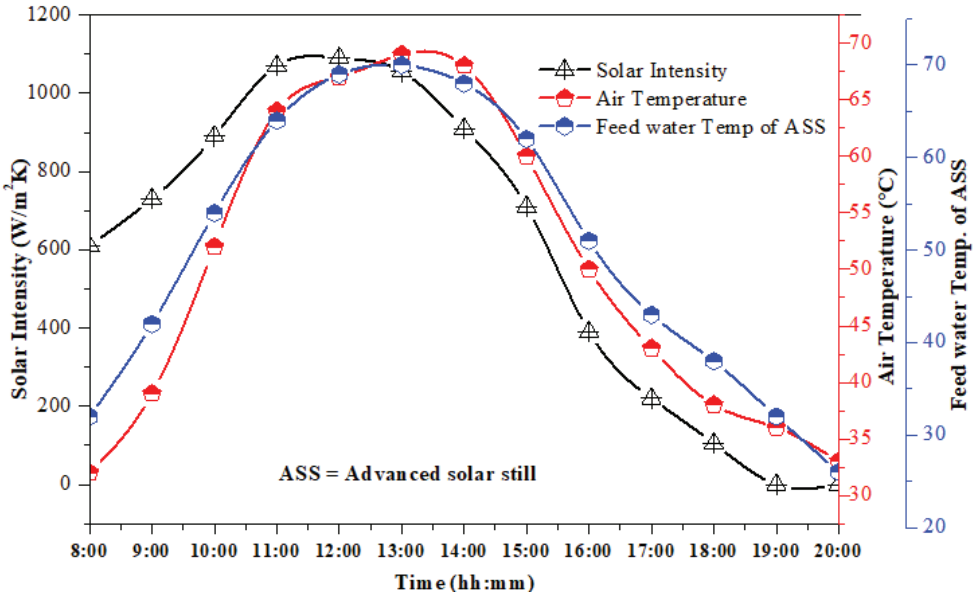

Figure 7. Variation in solar radiation, ambient temperature, and feed water temperature for CSS and ASS+EC.

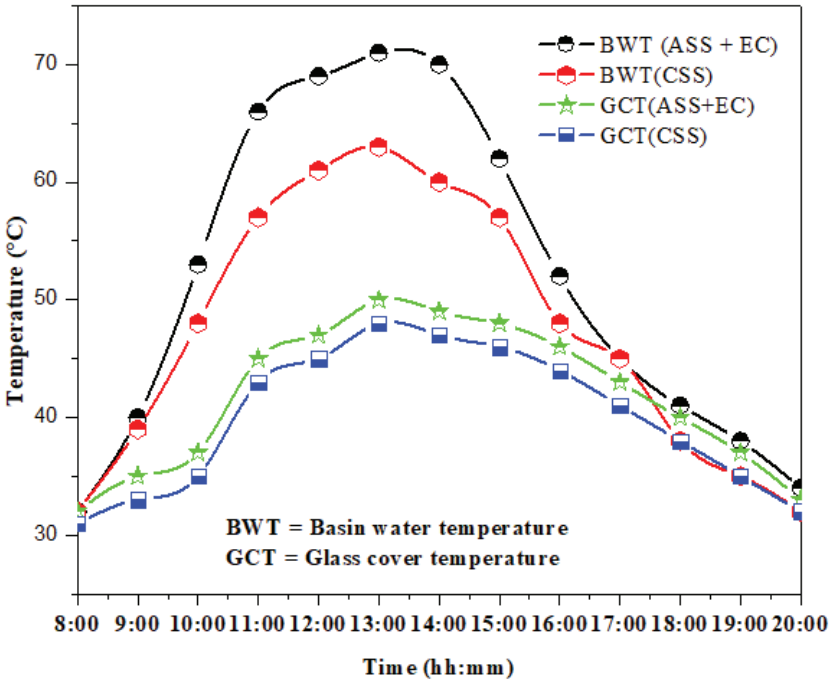

Figure 8. Variation in basin water and glass cover temperature for both systems.

Performance Analysis of ASS with Heating Coil and ZnO + PCM (ASS-PCM)

To improve productivity, a combination of phase change material (PCM) and ZnO nanoparticles was utilized as a thermal storage bed beneath the absorber plate of an active solar still (ASS). This setup was designed to enhance energy efficiency by leveraging the unique properties of the materials. The experiment incorporated a heating coil and PCM to lower the glass cover temperature, storing energy during periods of high solar intensity and releasing it when needed. The role of temperature in PCM is crucial for the charging and discharging processes, with energy stored as either sensible or latent heat, depending on the PCM's temperature relative to its melting point. Energy is stored during the charging phase and released during the discharging phase.

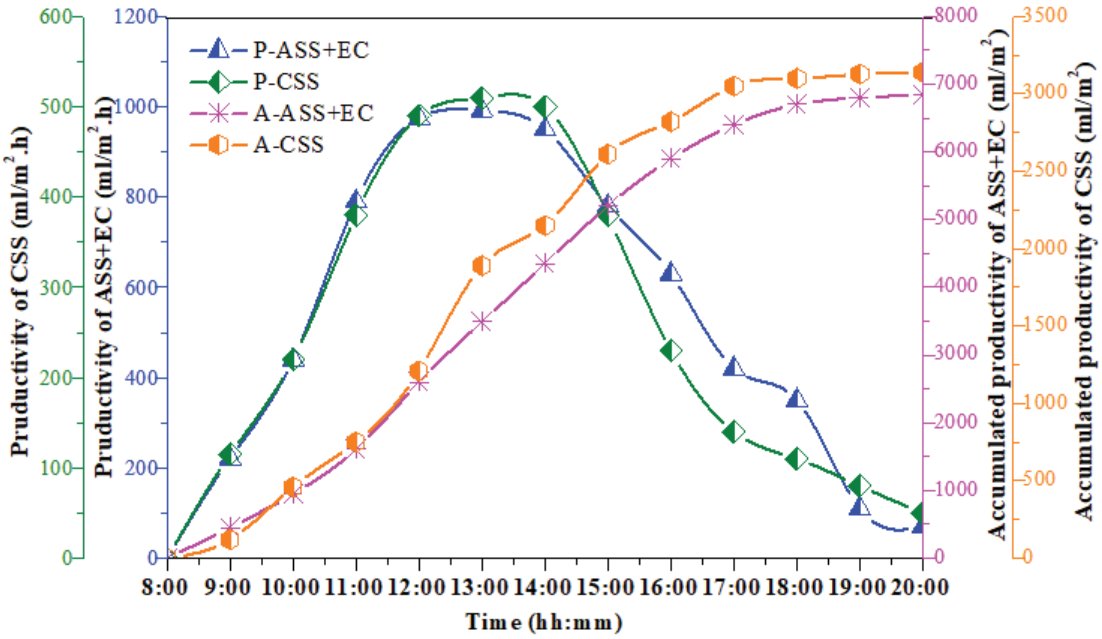

Figure 9. Hourly variation in productivity and accumulated productivity for ASS+EC and CSS.

Figure 10 displays the temperature changes of PCM and water for both the ASS-PCM and a conventional solar still (CSS). PCM with ZnO nanoparticles demonstrated superior thermal conductivity and lower melting and solidification temperatures compared to PCM without nanoparticles. The temperature data show a gradual increase from early morning until about 13:00 hours for both the water and PCM temperatures in ASS-PCM and CSS, followed by a decline. Heat transfer occurred from the absorber to the PCM before 13:00 hours and from the PCM back to the absorber afterward, as the PCM temperature dropped to match the ambient temperature. Figure 10 also highlights that the temperature difference between the water in ASS-PCM and CSS was more pronounced during the discharging period than during the charging period, due to the heat transfer from the PCM to the ASS-PCM absorber.

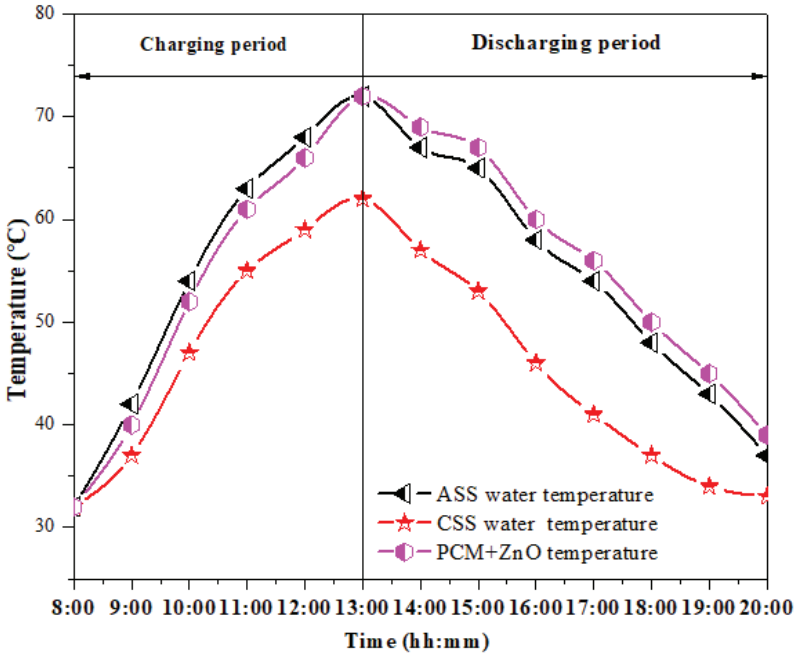

Figure 10. Variation in temperature for ASS, CSS, and ASS-PCM-ZnO.

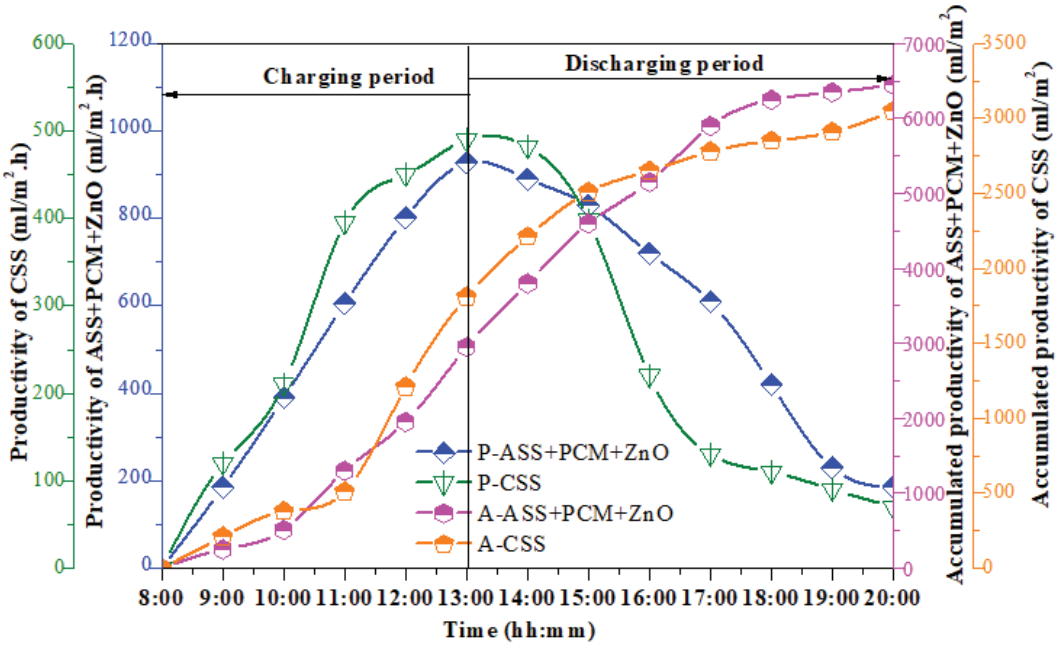

Figure 11. Representation of productivity and accumulated productivity.

Figure 11 presents the hourly and cumulative productivities for ASS-PCM and CSS. The trends indicate that ASS-PCM consistently performed more efficiently than CSS in terms of yield throughout the experiment. This efficiency is attributed to higher basin water temperature (BWT), evaporation, and condensation rates in ASS-PCM compared to CSS. The cumulative yield of ASS-PCM (6600 ml/m²) was nearly 113% higher than that of CSS (3090 ml/m²), as shown in Figure 11. Consequently, the productivity of ASS-PCM increased by about 36% due to the use of PCM.

Thermal Efficiency and Increased Yield of ASS

Thermal efficiency and freshwater yield are critical metrics in assessing the thermal performance of a solar still (SS) system. The improvement in productivity for an active solar still (ASS) compared to a conventional solar still (CSS) is illustrated in Figure 8 as a percentage increase. The thermal

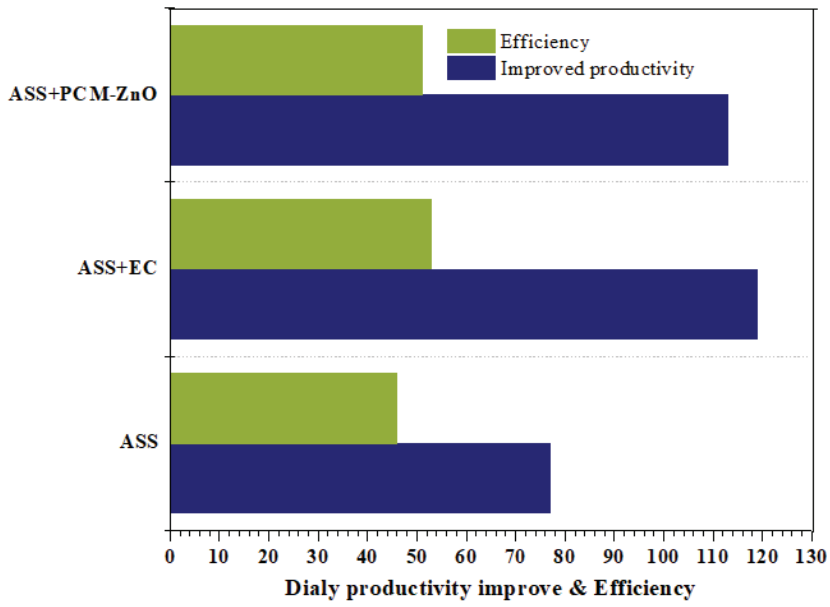

Figure 12. Relationship between daily productivity increase and efficiency.

Table 4. Fixed price of CSS and ASS

S.No.	Materials	CSS($)	ASS($)
1.	Steel sheet	22	22
2.	Glass cover	19	19
3.	Iron stand and ducts	24	24
4.	Production	25	41
5.	Wood	25	25
6.	Thermocol	0.36	0.36
7	Oil paint	10	10
8.	Float	04	04
9.	DC fan	-	28
10.	Copper tube for heating coil	-	12
11.	Phase change material	-	10
12.	ZnO Nanoparticles	-	30
13.	PV panel	-	43
14.	Silicone gel	5	5
15.	Labor cost	12	12

efficiency for each configuration is presented in Figure 12. The maximum thermal efficiency and corresponding yield improvements are quantified as follows: 46% and 77% for ASS with a heating coil, 53% and 119% for ASS with an external condenser (ASS-EC), and 51% and 113% for ASS with PCM-ZnO nanoparticles.

Cost Analysis

Fixed prices of both ASS and CSS with different modifications are listed in Table 4. Furthermore, assumptions (no. of working days in a year, interest rate, and system lifetime) and estimates for variables used in economic analysis are discussed in Table 5. Desalinated freshwater's acquired prices were correspondingly 0.030, 0.023, and 0.021 $/l for the CSS, ASS-PCM, and ASS-EC.

Environmental Analysis

Environmental analysis is crucial in assessing the impact of advanced solar still (ASS) systems on the environment.

Table 5. Price of different components

Factors	Mean	Value			Unit
		CSS	ASS-EC	ASS-PCM	
n	System lifetime	15	15	15	Years
i	Interest rate per annum	12	12	12	%
N	Workings days per annum	340	340	340	Day
P	Setup fixed price	146.36	245.36	269.36	$
M	Average production of desalinated water	1100	2450	2300	l/m^2 year
CPL	Price of desalinated water	0.030	0.021	0.023	$/l
AMC	Annual maintenance cost	2.30	3.80	3.85	$
ASV	Annual salvage value	0.55	0.92	0.93	$

Table 6. Embodied energy of used materials [10]

Materials used	Embodied Energy (kWh/kg)	Mass (kg)	Total Embodied Energy (kWh) CSS	Total Embodied Energy (kWh) ASS
Plywood (for structure)	10.5	10	105	105
Thermocol (for insulation)	89.0	0.25	22.25	22.25
Copper tube	19.85	5	00	99.25
Stainless steel	55.65	12.5	695.25	695.25
Al frame	165	0.25	41.25	41.25
Paint	91.01	0.25	22.75	22.75
Fitting materials(valve and nozzle)	56.12	2.1	117.85	117.85
DC fan made of plastic	19.54	0.4	00	7.816
Oil paint	25.25	2	50.5	50.5
PV panels	740	01 no.	740	740
ZnO nanoparticles	55	0.02	00	1.1
Electricity wire	19.59	0.1	1.959	1.959
Al T and L-shaped joint	55.25	26	1436.5	1436
Glass	15.9	8	127.2	127.2
Total embodied energy			**3360.014**	**3468.18**

Table 7. Equations used for calculation [41]

Eq. No.	Equations	Ref.
13.	$\text{Energy Payback Period} = \frac{\text{Emboided Energy } (E_e)}{\text{Annual Thermal Energy Output } (E_a)}$	[42]
14.	$CO_2 \text{ emission per year} = \frac{E_e}{L} \times 0.98 \text{ kg}$ $CO_2 \text{ emission per year} = \frac{E_e}{L} \times \frac{1}{1-L_a} \times \frac{1}{1-L_t} \times 0.98 \text{ kg}$ If $L_t = 0.40$ and $L_a = 0.20$ due to old appliances, then Eq. becomes as follows: $CO_2 \text{ emission per year} = \frac{E_e}{L} \times 2.042 \text{ kg}$	[42]
15.	$CO_2 \text{ mitigation per year} = E_{system} \times \frac{1}{1-L_a} \times \frac{1}{1-L_t} \times 0.98 \text{ kg}$ $CO_2 \text{ mitigation per year} = E_{system} \times 2.042 \text{ kg}$	[43]
16.	For a life span of N years, it would be $= E_{system} \times N \times \frac{1}{1-L_a} \times \frac{1}{1-L_t} \times 0.98 \text{ kg}$ For a life span of N years, it would be $= E_{system} \times N \times 2.042 \text{ kg}$	[43]
17.	Net CO_2 mitigation = Lifetime CO_2 mitigation - Lifetime CO_2 emission $= (E_{system} \times N - E_e) \times \frac{1}{1-L_a} \times \frac{1}{1-L_t} \times 0.98\text{kg}$ $= (E_{system} \times N - E_e) \times 2.042\text{kg}$	[42]

Table 8. Outcomes of environmental parameters

Environmental factors	Unit	CSS	ASS
EBPT	Year	2.20	2.50
Carbon Credit Earned	$	6525.58	7520.12
CO_2 Emitted	kg/year	68.25	145.25
CO_2 Mitigation	kg/year	475.25	960.31
Net CO_2 Mitigation (Lifetime)	Tons	6.10	8.12

Solar still systems are exemplary sustainable solutions that have no adverse effects on the atmosphere. The first step in this analysis is to calculate the embodied energy for both advanced and conventional solar stills. Table 6 details the embodied energy for various materials used in the fabrication of both systems. The assumptions and calculations used in the environmental analysis are outlined in Table 7. Key metrics calculated include Embodied Energy Payback Time (EBPT), CO_2 mitigation, carbon credit earned, CO_2 emitted, and net CO_2 mitigation over the system's lifetime (Table 8).

CONCLUSION

The experimentation was conducted to compare the thermal performance, efficiency, and productivity of potable water between conventional solar stills and advanced solar stills (including variations with a heating coil, external condenser, and ZnO-PCM) under identical meteorological conditions. A copper heating coil was installed in the back wall of the solar still to enhance the feed water temperature, improve the condensation process, and lower the back wall temperature of the solar still.

The results yielded the following conclusions:

1. The cumulative yield of advanced solar stills (5500 ml/m². day) was nearly 77% higher than that of CSS (3090 ml/m². day).
2. The yield of freshwater at 13:00h was 7000 ml/m². day for advanced solar stills - external condenser and 3200 ml/m². day for conventional solar stills. Thus, advanced solar stills using - an external condenser produced 119% more distillate than conventional ones, resulting in a productivity increase of about 42% for advanced solar stills external condenser.
3. The cumulative yield of advanced solar stills-PCM (6600 ml/m². day) was approximately 113% higher than conventional solar stills (3090 ml/m². day), as shown in Figure 11. Consequently, the productivity of advanced solar stills-PCM increased by about 36% with the use of PCM.
4. The maximum thermal efficiency and improved yield were 46% & 77% for advanced solar stills with a heating coil, 53% & 119% for advanced solar stills with - an external condenser, and 51% & 113% for advanced solar stills with ZnO-PCM, respectively.
5. CO_2 emissions depend on the embodied energy of the materials fabricating the solar still system. Since advanced solar stills includes auxiliary devices compared to conventional solar stills, CO_2 emissions are 52.83% higher in advanced solar stills.

The high thermal conductivity of ZnO nanoparticles offers great potential for enhancing heat transfer in the desalination system. Future developments could explore the use of advanced nanomaterials like ZnO in combination with other nanoparticles to achieve even greater thermal efficiency, which would result in faster water evaporation and higher desalination rates. As solar desalination technology evolves, integrating PCMs and ZnO nanoparticles could make off-grid, self-sustaining desalination systems more practical for remote, water-scarce regions. These systems could be powered solely by renewable energy, making them ideal for regions with limited infrastructure, such as islands, deserts, or rural communities.

NOMENCLATURE

A	area of the system (m^2)
ASS	Advanced solar still
CSS	Conventional solar still
EC	External condenser
HC	Heating coil
h_{fg}	latent heat of vaporization,
I	average solar intensity
i	interest per annum (assumed 12%),
L_a	appliances losses
L_t	transmission losses
m	hourly distillate
m_w	Mass of water (ml)
m_{np}	Mass of nanoparticles (gm)
n	no. of life in years
PCM	Phase change material
P_F	DC fan power
SS	Solar still
S	salvage value of the system after n years
T_w	Temperature of water (°C)

Greek symbols

η_d	daily thermal efficiency %
φ_{np}	Concentration of nanoparticles

AUTHORSHIP CONTRIBUTIONS

Authors equally contributed to this work.

DATA AVAILABILITY STATEMENT

The authors confirm that the data that supports the findings of this study are available within the article. Raw data that support the finding of this study are available from the corresponding author, upon reasonable request.

CONFLICT OF INTEREST

The author declared no potential conflicts of interest with respect to the research, authorship, and/or publication of this article.

ETHICS

There are no ethical issues with the publication of this manuscript.

REFERENCES

[1] Al-Qasaab MR, Abed QA, Abd Al-wahid WA. Enhancement the solar distiller water by using parabolic dish collector with single slope solar still. J Therm Eng 2021;7:1001–1015. [CrossRef]

[2] Almahdawi YA, Abbas MK, Al-Samari A, Aldabash N, Hafedh SA. Temperature effect in the energy degradation of photovoltaic power. J Therm Eng 2023;9:1153–1162. [CrossRef]

[3] Younes MM, El-Sharkawy II, Kabeel AE, Uddin K, Miyazaki T, Saha BB. Characterization of silica gel-based composites for adsorption cooling applications. Int J Refrig 2020;118:345–353. [CrossRef]

[4] Younes MM, El-Sharkawy II, Kabeel AE, Saha BB. A review on adsorbent-adsorbate pairs for cooling applications. Appl Therm Eng 2017;114:394–414. [CrossRef]

[5] Ward J. A plastic solar water purifier with high output. Sol Energy 2003;75:433–437. [CrossRef]

[6] Kabeel AE, Khalil A, Omara ZM, Younes MM. Theoretical and experimental parametric study of modified stepped solar still. Desalination 2012;289:12–20. [CrossRef]

[7] Younes MM, Abdullah AS, Essa FA, Omara ZM. Half barrel and corrugated wick solar stills – Comprehensive study. J Energy Storage 2021;42:103117. [CrossRef]

[8] Saravanan A, Murugan M. Performance evaluation of square pyramid solar still with various vertical wick materials – An experimental approach. Therm Sci Eng Prog 2020;19:100581. [CrossRef]

[9] Farouk WM, Abdullah AS, Mohammed SA, Alawee WH, Omara ZM, Essa FA. Modeling and optimization of working conditions of pyramid solar still with different nanoparticles using response surface methodology. Case Stud Therm Eng 2022;33:101984. [CrossRef]

[10] Gaur MK, Thakur VK. Experimental analysis of sustainability of passive solar still with nanoparticles operating at various angles of glass cover. Energy Sources Part A Recover Util Environ Eff 2022;44:5227–5245. [CrossRef]

[11] Anshika R, Suresh S, Anil K. Review on thermal modeling of solar desalination systems. Res J Chem Environ 2019;23:90–102.

[12] Tiwari S, Rathore PKS. Performance enhancement of solar still for water desalination integrated with thermal energy storage. Mater Today Proc 2023;74:202–206. [CrossRef]

[13] Prakash O, Ahmad A, Kumar A, Hasnain SMM, Kumar G. Comprehensive analysis of design software application in solar distillation units. Mater Sci Energy Technol 2022;5:171–180. [CrossRef]

[14] Abdullah AS, Younes MM, Omara ZM, Essa FA. New design of trays solar still with enhanced evaporation methods – Comprehensive study. Sol Energy 2020;203:164–174. [CrossRef]
[15] Thakur VK, Gaur MK, Dhamneya AK, Chaurasiya PK. Validation of thermal models to predict the productivity and heat transfer coefficients for passive solar still with different nanoparticles. Energy Sources Part A Recover Util Environ Eff 2021:1971338. [CrossRef]
[16] Dharamveer, Samsher, Kumar A. Analytical study of photovoltaic thermal compound parabolic concentrator active double slope solar distiller with a helical coiled heat exchanger using CuO nanoparticles. Desalin Water Treat 2021;233:30–51. [CrossRef]
[17] Kumar A, Vyas S, Nkwetta DN. Experimental study of single slope solar still coupled with parabolic trough collector. Mater Sci Energy Technol 2020;3:700–708. [CrossRef]
[18] Kant R, Kumar A. Process optimization of conventional steam distillation system for peppermint oil extraction. Energy Sources Part A Recover Util Environ Eff 2022;44:3960–3980. [CrossRef]
[19] Kant R, Kumar A. Thermodynamic analysis of solar assisted steam distillation system for peppermint oil extraction. J Food Process Eng 2023;46:e14228. [CrossRef]
[20] Murugavel KK, Srithar K. Performance study on basin type double slope solar still with different wick materials and minimum mass of water. Renew Energy 2011;36:612–620. [CrossRef]
[21] Abdullah AS, Omara ZM, Ben Bacha H, Younes MM. Rotating-drum solar still with enhanced evaporation and condensation techniques: Comprehensive study. Energy Convers Manag 2019;199:112024. [CrossRef]
[22] Ketabchi F, Gorjian S, Sabzehparvar S, Shadram Z, Ghoreishi MS, Rahimzadeh H. Experimental performance evaluation of a modified solar still integrated with a cooling system and external flat-plate reflectors. Sol Energy 2019;187:137–146. [CrossRef]
[23] Abdullah AS, Omara ZM, Ben Bacha H, Younes MM. Employing convex shape absorber for enhancing the performance of solar still desalination system. J Energy Storage 2022;47:103573. [CrossRef]
[24] Yassen TA, Al-Kayiem HH. Experimental investigation and evaluation of hybrid solar/thermal dryer combined with supplementary recovery dryer. Sol Energy 2016;134:284–293. [CrossRef]
[25] Aktaş M, Khanlari A, Amini A, Şevik S. Performance analysis of heat pump and infrared–heat pump drying of grated carrot using energy-exergy methodology. Energy Convers Manag 2017;132:327–338. [CrossRef]
[26] Lisboa AAV, Segurado R, Mendes MAA. Solar still performance for small-scale and low-cost seawater desalination: Model-based analysis and water yield enhancement techniques. Sol Energy 2022;238:341–362. [CrossRef]
[27] Dumka P, Sharma A, Kushwah Y, Raghav AS, Mishra DR. Performance evaluation of single slope solar still augmented with sand-filled cotton bags. J Energy Storage 2019;25:100888. [CrossRef]
[28] Dumka P, Mishra DR. Comparative experimental evaluation of conventional solar still (CSS) and CSS augmented with wax-filled metallic finned-cups. FME Trans 2020;48:482–495. [CrossRef]
[29] Panchal H, Hishan SS, Rahim R, Sadasivuni KK. Graphite powder mixed with black paint on the absorber plate of the solar still to enhance yield: An experimental investigation. Desalination 2021;520:115349. [CrossRef]
[30] Panchal H, Hishan SS, Rahim R, Sadasivuni KK. Solar still with evacuated tubes and calcium stones to enhance the yield: An experimental investigation. Process Saf Environ Prot 2020;142:150–155. [CrossRef]
[31] Murugan M, Vijayan R, Saravanan A, Jaisankar S. Performance enhancement of centrally finned twist inserted solar collector using corrugated booster reflectors. Energy 2019;168:858–869. [CrossRef]
[32] Alawee WH, Mohammed SA, Dhahad HA, Essa FA, Omara ZM, Abdullah AS. Performance analysis of a double-slope solar still with elevated basin—comprehensive study. Desalin Water Treat 2021;223:13–25. [CrossRef]
[33] Elamy MI, Mohammed SA, Basem A, Alawee WH, Abdullah AS, Aldabesh A, et al. Enhancing coiled solar still performance with vertical wick distiller, reflectors, nanomaterial-infused PCM, and condenser integration. Case Stud Therm Eng 2024;61:104912. [CrossRef]
[34] Younes MM, Abdullah AS, Omara ZM, Essa FA. Enhancement of discs' solar still performance using thermal energy storage unit and reflectors: An experimental approach. Alexandria Eng J 2022;61:7477–7487. [CrossRef]
[35] Nakade A, Aglawe A, More K, Kalbande VP. Experimental analysis of two-stage solar still integrated with thermal storage based solar collector using nano-enhanced phase change materials. Desalin Water Treat 2024;320:100755. [CrossRef]
[36] Omara ZM, Kabeel AE, Younes MM. Enhancing the stepped solar still performance using internal reflectors. Desalination 2013;314:67–72. [CrossRef]
[37] Abdullah AS, Omara ZM, Essa FA, Younes MM, Shanmugan S, Abdelgaied M, et al. Improving the performance of trays solar still using wick corrugated absorber, nano-enhanced phase change material and photovoltaics-powered heaters. J Energy Storage 2021;40:102782. [CrossRef]
[38] Abdullah AS, Essa FA, Ben Bacha H, Omara ZM. Improving the trays solar still performance using reflectors and phase change material with nanoparticles. J Energy Storage 2020;31:101744. [CrossRef]

[39] Kushwah A, Kumar A, Gaur MK. Drying kinetics, performance, and quality assessment for banana slices using heat pump–assisted drying system (HPADS). J Food Process Eng 2022;45:1–10. [CrossRef]

[40] Alawee WH, Abdullah AS, Mohammed SA, Majdi A, Omara ZM, Younes MM. Testing a single slope solar still with copper heating coil, external condenser, and phase change material. J Energy Storage 2022;56:106030. [CrossRef]

[41] Yadav S, Chandramohan VP. Numerical analysis on thermal energy storage device with finned copper tube for an indirect type solar drying system. J Sol Energy Eng Trans 2018;140:1–13. [CrossRef]

[42] Prakash O, Kumar A. Environomical analysis and mathematical modelling for tomato flakes drying in a modified greenhouse dryer under active mode. Int J Food Eng 2014;10:669–681. [CrossRef]

[43] Singh P, Gaur MK. Environmental and economic analysis of novel hybrid active greenhouse solar dryer with evacuated tube solar collector. Sustain Energy Technol Assess 2021;47:101428. [CrossRef]